Experimental Whole-Body Average SAR Estimation System using Cylindrical Field Scanning Method

Yoshifumi Kawamura, Takashi Hikage, Toshio Nojima

Graduate school of Information Science and Technology, Hokkaido University
Kita 14, Nishi 9, Kita-ku, Sapporo, Hokkaido, 060-0814 Japan
{kawamura, hikage, nojima}@wtemc.ist.hokudai.ac.jp

Abstract — **This paper presents a new whole-body averaged specific absorption rate (SAR) estimation method based on the cylindrical fields scanning technique. The aim of this study is to achieve experimentally an estimation of whole-body averaged SAR in human models due to plane wave exposure using the radiation-field scanning technique. In this paper, the validity of the proposed methods is investigated using Finite-difference time-domain (FDTD) calculations for the purpose of design and development of the experimental system. The calculated whole-body averaged SAR based on the proposed method is compared with that obtained by conventional estimation methods.**

Key words: Whole-Body Averaged SAR, Scaled model, Mobile phone frequency, Plane-wave exposure system.

I. INTRODUCTION

A basic guideline used as the reference value of biological effects is a whole-body averaged specific absorption rate (SAR). A numerical analysis including high accuracy human models has become possible using computer software. Previously, in order to estimate the biological effects, several organizations have carried out precise numerical simulations [1-3] and experimental measurements [4, 5].

Generally, the SAR experimental measurements apply 3-D scanning techniques using electric probes or thermo graphic techniques. However, experimental evaluation that correlates to computer presumption of the whole-body averaged SAR has not been carried out sufficiently. Therefore, in this paper, we propose an experimental measurement method that can be used to acquire measurement data. This method measures electric field strength by scanning a cylindrical surface used when the radiation pattern of the antenna is presumed [6, 7], and presumes that the electric power radiated from the poynting vector is calculated from the electric field data.

In this paper, a new numerical calculation method of whole-body averaged SAR is shown. Then, after showing the numerical analysis model of the experiments, the proposed method is applied to this simulation model. To confirm the validity of the proposed technique, we compare the whole-body averaged SAR of the proposed method with results obtained using the conventional FDTD (Finite-difference Time-domain) calculation method.

II. PROPOSED WHOLE-BODY SAR ESTIMATION METHOD

A. Absorbed Power Estimation Method

The whole-body averaged SAR is obtained by a value of SARs averaged over the whole body. Basically, this technique has been used to measure physical models having liquids similar to living bodies. This technique is not suited for experimental measurement that is intended for biological tissues, because it should measure the electric field in the part of in vivo through the electric field probes.

Then, a novel whole-body averaged SAR method is proposed. It is a technique for presuming whole-body averaged SAR by measuring the radiation electric power of the closed surfaces including the biological tissues. This method is a measurement technique of scanning the electromagnetic field data in the near-field of the antenna when the radiation characteristic of the antenna is measured [6]. In this method, the absorbed power (W_{ab}) of the measurement lossy material is derived from measuring the radiation power in a closed arbitrary space (W_{out}) and an antenna output electric power (W_{in}).

The radiation power of the close space uses poynting vector $\boldsymbol{S}$ (in watts per square meter) based on the electric field strength data obtained with each measurement point.

$$\mathbf{S} = \frac{1}{2}\mathbf{E} \times \mathbf{H}^* \qquad (1)$$

Thus, $\boldsymbol{E}$ (in volts per meter) is shown a complex electric field and $\boldsymbol{H}$ (in amperes per meter) is shown a complex magnetic field. Hence, the complex poynting vector can presume this from showing the electric power radiated from an arbitrary side for a general medium, and the radiation electric power of the close space is presumed by the area (surface integral) as follows:

$$W_{out} = \oint_S \mathbf{S} \cdot \mathbf{n} dS \qquad (2)$$

The absorbed power of the lossy material is obtained by the following expression:

$$W_{ab} = W_{in} - W_{out} \qquad (3)$$

Moreover, the whole-body averaged SAR can be derived from the absorbed power (W_{ab}) and weight of the lossy material as follows:

$$\text{Whole-body averaged SAR} = \frac{W_{ab}}{\text{Weight}} \qquad (4)$$

B. Field scanning method

Three major approaches have been used for scanning the electromagnetic field data. The types of scanning surfaces used are the planar, cylindrical and spherical surfaces. The advantages and disadvantages of using the different surfaces have been previously discussed [6]. The scanning technique that is generally in use is spherical scanning. Spherical scanning makes high accuracy measurements possible since it can obtain the electromagnetic fields which are measured at the same length from the center position of scanning surfaces. However, it is not suited for the experimental system of whole-body averaged SAR since this system requires an increase in the estimation space and for the measured object to be suspended in midair.

On the other hand, cylindrical scanning and planar scanning are suited to this experiment system that is constructed. In this paper, the application of cylindrical scanning which is rotated to the experimental system is examined. In order to include areas not usually considered, such as the upper and lower parts of the cylinder, the absorbed power is subtracted from the radiation power when the lossy material is in the scanning surface as well as when the material is not in the scanning surface. Equation (2) is redefined (for cylindrical scanning) as follows:

$$W_{out} = \oint_S \mathbf{S} \cdot \mathbf{n} dS = \sum_{dz=0}^{Nz} \sum_{dp=0}^{Np} Sr \ dS \qquad (5)$$

III. Numerical Analysis

A. Scaled model

In order to generate uniform plane-wave excitation to the human body in the cellular phone frequency band (2.1 GHz), a large-scale evaluation area (of the order of 10's of meters) is required. Then, the evaluation area is reduced by scaling the size of the antenna and the frequency.

In the evaluation system including lossy materials such as human bodies, the condition requires that both the electric constant and the scale of the lossy material change. The reduced scale relation between the full-scale model and a model with a scale factor of k [8, 9] is shown in Table 1. In this paper, a 1/2 scale model is used.

Table 1: Electrical properties for full scale model and scale model

Parameter	Full scale model	Scale model
Length	l	$l' = kl$
Frequency	f	$f' = (1/k)f$
Permittivity	ε	$\varepsilon' = \varepsilon$
Conductivity	σ	$\sigma' = k\sigma$

B. Plane-wave exposure system

In order to easily generate a plane-wave with a sharp directivity, horn antennas with a sharp directivity are used as radiators. Figure 1 illustrates the plane-wave radiation system that was used. Only an arbitrary part of the human phantom is exposed since electric wave strength in the direction of the straight line of the horn antenna is high. Then, the radiating elements are assumed to be compositions with reasonable horizontal and vertical spacing and are parallel to each other. The horn antenna sources all have the same phase and amplitude. Moreover, to reduce the interference between horn antennas and to generate the plane wave over a short distance, a dielectric lens is designed and setup in front of the horn antenna.

The horn antenna used is a double ridge horn antenna in order to give the wideband characteristic. The overall size of the radiation system is 800×750×1300 mm. The radiation system irradiates a plane-wave in an area of 1000×500 mm that is 1000 mm away from the dielectric lens.

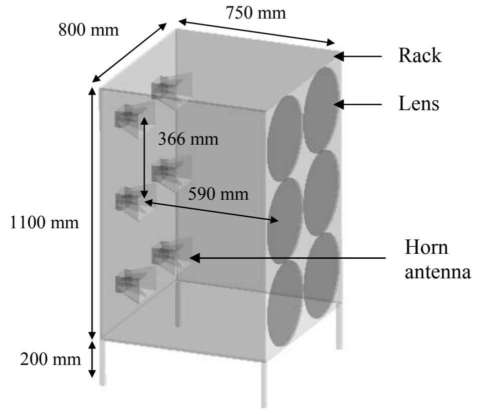

Figure 1: Prototype Plane-wave radiation system.

C. Phantom model

The numerical human model is shown in figure 2. This model is an enhanced high-resolution magnetic resonance imaging whole-body human model which was made by the Virtual Family Product [10]. This is a 34-year-old male adult. It is composed of 75 inhomogeneous tissues, and its height is about 1.74 m and 70 kg in weight. The resolution of the model used is 2 mm, and this is divided into cells of varying widths.

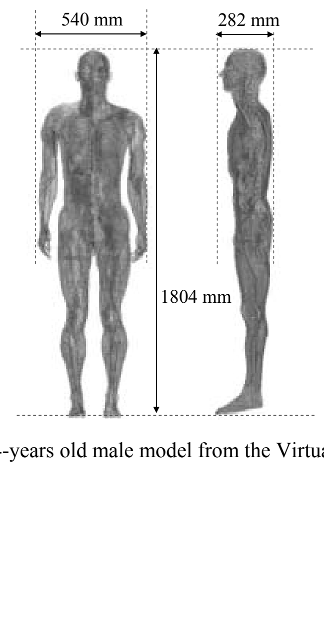

Figure 2: 34-years old male model from the Virtual Family.

D. Numerical Analysis model

The numerical electromagnetic field analysis is performed using the Finite-Difference Time-Domain (FDTD) method [11] since this method is better suited for the computation of large scale and high precision inhomogeneous programs. The FDTD numerical analysis is performed by commercial software SEMCAD X [12] which incorporates a number of advanced tools for the visualization and treatment of simulation results. The numerical model of the SAR experiment evaluation system including the numerical human model is shown in Figure 3.

This calculation model assumes that a plane wave generated by a 2.1GHz cellular phone is exposed to the human body. Since a 1/2 scale factor is taken, the objects in the model are reduced to 1/2 size and the antenna radiation frequency is 4.2GHz

The numerical human model that is used is a 1/2 scale model of a 34-year old adult male. The human model is composed of 2/3 muscle-equivalent tissue [13]. The human model is divided into cells with a minimum size of 1.0 mm and a maximum size of 1.5 mm in consideration of the effect of the wavelength short-circuit.

The horn antenna is composed of Perfect Electric Conductor (PEC), and fed delta gap source to the ridge part. The dielectric lens follows the design value. The horn antennas and the dielectric lenses are placed at intervals of 2.0 mm (maximum).

The arrangement of each object in the model is described as follows: The plane wave irradiation system and the numerical human model were separated by 1.0 m with the human model facing the irradiation system. Both the irradiation system and the human model are arranged such that they are at least two wavelengths from the absorbing boundary condition in order to apply the proposed evaluation method.

E. Validation of Planar scanning

In order to confirm that the field scanning method of free space is correct, the radiation power of the plane wave radiation system is estimated using the simplified planar scanning method. The poynting vector distribution of planar scanning is shown in Figure 4. These distribution results are shown as the components of the individual axes. The radiation power of the irradiation equipment is 6 W. The sampling intervals are 20 mm×20 mm.

The estimation result of the radiation power using planar scanning is 5.926 W. When compared to the input power of the irradiation equipment, the difference is within 1.3%. Thus, the validity of the field scanning has been confirmed.

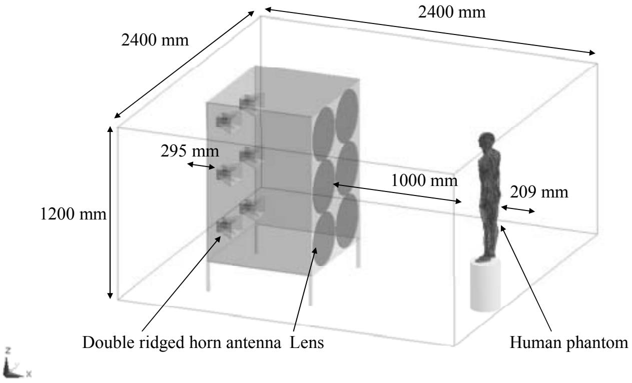

Figure 3: Numerical analysis model.

Table 3 Computation Parameters.

Frequency	4200 MHz
Cell size	1 mm (minimum) 7 mm (maximum)
Iteration	150 Periods
Absorbing Boundary Condition	U-PML (8 Layers)
Total Program size	548 x 698 x 763 (290 MCells)
Material	Human Phantom: ε_r 39.82, σ 2.98, ρ 1000kg/m^3 Dielectric Lens: ε_r 4.0 Rack(Air): ε_r 1.0 Metal: PEC

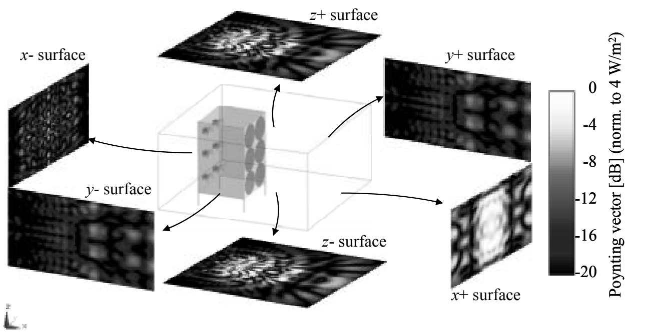

Figure 4: Poynting vector distribution of planar scanning (without human phantom)

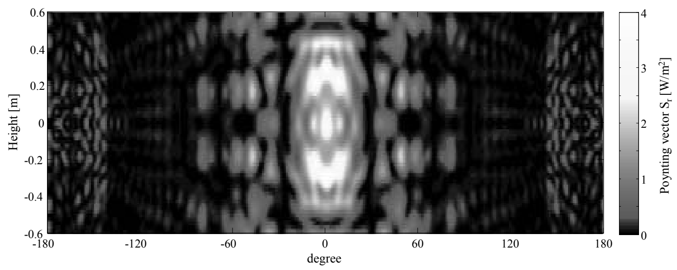

Figure 5: Poynting vector (Sr) distribution of cylindrical scanning (including human phantom). 0 degrees represents the position behind the human phantom and 180 degrees represents the position behind the plane-wave radiation system.

IV. RESULT

The analytical results of the FDTD technique have been presented. The antenna input impedance of the plane-wave radiation system is 122 + j18.9 Ω and 121 + j22.9 Ω when the human phantom is present and absent respectively. From this, it is understood that the exposure object does not influence the characteristic of the antenna. The total radiation electric power of the irradiation system was 6 W. Thus, the electric power density of the plane wave excitation space of the irradiation equipment became about 4 W/m^2.

Next, the poynting vector in four corners was derived based on the electromagnetic field data. The poynting vector was sampled so that the length of the arc of 'θ' and 'z' may become about 20 mm on all sides. This length of 20 mm is about 1/4 of one wavelength (71.4 mm) for 4.2 GHz. The electric power radiated from the cylindrical scanning area is evaluated from the poynting vector data. The Poynting vector distribution of cylindrical scanning result is shown in Figure 5. The center of an analytical area is made the starting point, and the evaluation side is made the side of a cylinder with height 1.2 m and diameter 2.4 m. Figure 5 shows the height of the spindle and a horizontal axis and the angle from the starting point is shown. The horizontal axis assumes the rear side of human and the radiation system is assumed to be at 0 degrees and 180 degrees, respectively.

The human body model's absorbed power and whole-body averaged SAR continuously requested according to the area of the poynting vector are shown in Table 3. The SAR obtained by conventional calculation is also shown for the comparison. The whole-body averaged SARs are calculated using the weight of scaled human phantom model (8.549 kg) as derived from the original model (70 kg). The numerical result of whole-body averaged SAR is 0.026 W/kg in this proposal technique and 0.020 W/kg in the conventional calculation method. It can be confirmed that it is possible to derive the averaged SAR of the whole body by using the proposed method. However, with this proposal technique, an increase of about 29.7% is expected when compared with conventional calculations for whole-body averaged SAR.

Table 3 Absorbed power and SAR Estimation result

Parameter	Proposed method	Conventional calculation method
W_{ab} [W]	0.227	0.175
WB SAR [W/kg]	0.026	0.020
Variation	+ 29.7 %	

V. CONCLUSIONS

Based on the cylindrical radiation-field scanning technique, a new whole-body averaged SAR estimation method that is appropriate for developing the experimental evaluation system is proposed. In the case of cylindrical scanning, the area that can be modeled is limited, and this was clarified to be the cause of the error margin of 29.7% when compared with the result of the conventional estimation method. This variation is caused by a decrease in the radiation electric power obtained by cylindrical scanning, since the cylindrical scanning area has a minimum height. We consider that the variation is improved when the height of the cylindrical scanning area increases. The proposal technique will be applied in the case where a large-scale numerical analysis that uses a detailed model is done, and the accuracy when the sampling on the electric power evaluation area is improved will be evaluated in the near future. Moreover, the actual experiment system that is shown in this paper will be constructed, and the validity of this proposal technique can then be confirmed.

ACKNOWLEDGMENTS

This work is supported by Grant-in-Aid from the Ministry of Internal Affairs and Communications (MIC) of Japan.

REFERENCES

[1] P J Dimbylow, "Fine resolution calculations of SAR in the human body for frequencies up to 3 GHz," Phys. Med. Biol, vol. 47, pp. 2835-2846, 2002.

[2] E. Conil, A. Hadjem, F. Lacroux, M F Wong and J Wiart, "Variability analysis of SAR from 20 MHz to 2.4 GHz for different adult and child models using finite-difference time-domain," Phys. Med. Biol, vol. 53, pp. 1511-1525, 2008.

[3] J. Wang, O. Fujiwara, S. Kodera and S. Watanabe, "FDTD calculation of whole-body average SAR in adult and child models for frequencies from 30 MHz to 3 GHz," Phys. Med. Biol, vol. 51, pp. 4119-4127, 2006.

[4] Y. Okano, K. Ito and H. Kawai, "Solid Phantom Composed of Glycerin and its Application to SAR Estimation," IEICE Trans. Commun, J83-B, no.4, pp.534-543, 2000.

[5] A. W. Guy, C.-K. Chou and B. Neuhaus, "Average SAR and SAR Distributions in Man Exposured to 450-MHz Radiofrequency Radiation," IEEE Trans. Microw. Theory Tech., vol. MTT-32, no. 8, pp. 452-762, 1984

[6] "Antenna Measurement Techniques," 1990

[7] J. A-Hansen, "On Cylindrical Near-Field Scanning Techniques," IEEE Trans. Antenna Propagat., vol. AP-28, pp. 231-234, March 1980.

[8] A. Miyata, Y. Yokota, K. Fujimoto and T. Maeda, "A Proposal of UWB Scale-Up Model Phantoms for the Scale Model Evaluations of UWB Antennas Including the Effects of Human Body," IEICE Trans. Commun., J91-B, no.7, 801-805, 2008.

[9] C.A. Balanis, Antenna Theory: Analysis and Design, 3rd ed., pp1044-1045, Wiley-Interscience, 2005.

[10] Christ A., Kainz W., Hahn, E., Honegger K., Shen J., Rascher W., Janka R., Bautz W., Kiefer B., Schmitt P., Hollenbach H., Chen J., Kam A., Neufeld E., Oberle M. and Kuster N., "The Virtual Family Project - Development of Anatomical Whole-Body Models of Two Adults and Two Children," Proceedings of the 23rd Annual Review of Progress in Applied Computational Electromagnetics (ACES) 2007, 2007.

[11] A.Taflove, "Computational Electrodynamics (The Finite-Difference Time-Domain Method)," Artech House, Boston, 1995.

[12] Schmid & Partner Engineering AG, SEMCAD-X (http://www.semcad.com)

[13] C.Gabriel, "Compilation of the dielectric properties of body tissues at RF and microwave frequencies," Brooks Air Force Technical Report AL/OE-TR-1996-0037, 1996.